

Supporting Information

Pressure-Dependent Growth of Wafer-scale Few-Layer h-BN by Metal-Organic Chemical Vapor Deposition

Dong Yeong Kim[†], Nam Han[†], Hokyong Jeong[†], Jaewon Kim[†], Sunyong Hwang[†],

Kyung Song[‡], Si-Young Choi[‡], and Jong Kyu Kim^{,†}.*

[†]Department of Materials Science and Engineering, Pohang University of Science and Technology (POSTECH), Pohang, 37673, Republic of Korea

[‡] Materials Modeling and Characterization Department, Korea Institute of Materials Science (KIMS), Changwon, 51508, Republic of Korea

Supporting Information S1. XRR spectrum

1) Thickness calculation from the XRR data

Film thickness is deduced by fitting the experimental XRR data through the following process. First, measured intensity I_{measured} is normalized by considering geometric factor since there is loss in the intensity of the incident X-ray at the low angle.

$$I_{\text{normalized}} = I_{\text{measured}} \frac{\sin(\theta_B)}{\sin(\theta)}$$

where, θ is the incident angle of the X-ray and θ_B is the incident angle when illuminated area of X-ray matches the sample size.

Second, the scattering vector of the X-ray along the surface normal direction, Q_z , is calculated from θ as

$$Q_z = k_f - k_i = 4\pi \frac{\sin(\theta)}{\lambda}$$

where, k_f and k_i are the wave vectors of the scattered and incident X-ray, respectively, and λ is the wavelength of the X-ray. Figure S1-1 shows the raw and corrected XRR spectrum as a function of θ and Q_z , respectively.

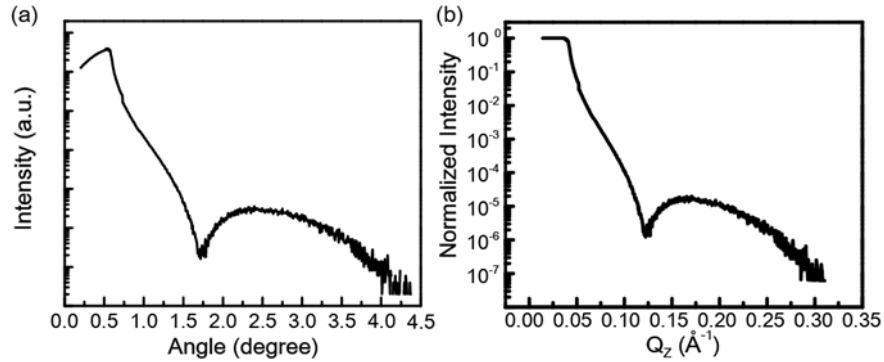


Figure S1-1. (a) Raw XRR spectrum as a function of θ and (b) corrected XRR spectrum as a function of Q_z .

Then, the XRR spectrum is fitted by Parratt32 which is software calculating the optical reflectivity of X-ray from flat surface using following formula^{S1}:

Wave vector inside layer n :

$$k_{z,n} = \sqrt{k_{z,0}^2 - 4\pi\rho_n}$$

where, ρ is scattering length density.

Fresnel coefficient at n^{th} interface:

$$r_{n,n+1} = \frac{k_{z,n} - k_{z,n+1}}{k_{z,n} + k_{z,n+1}} \exp[-2\sigma_{n+1}^2 k_{z,n} k_{z,n+1}]$$

where σ is a parameter describing the surface roughness.

Reflectivity of n^{th} layers from the Fresnel reflection:

$$R_n = \frac{r_{n,n+1} + R_{n+1} \exp[2id_{n+1}k_{z,n+1}]}{1 + r_{n,n+1}R_{n+1} \exp[2id_{n+1}k_{z,n+1}]}$$

where $r_{n,n+1}$ is the Fresnel coefficient at n^{th} interface described above, and d_n is the thickness of n^{th} layer. For the recursive calculation involving R_n and R_{n+1} , incident wave is normalized to unity and reflection from the substrate is ignored.

The layer's parameters including thickness are optimized to reproduce the measured XRR spectrum data. The accuracy of the fitting result is evaluated by the least square method.

2) Thickness uniformity

Figure S1-2 is the XRR spectra of the MOCVD-grown h-BN measured at six different positions in a single 2-inch sapphire wafer. The calculated thickness for this film is 3.545 ± 0.133 nm, and it shows the wafer-scale thickness uniformity of the MOCVD-grown h-BN film.

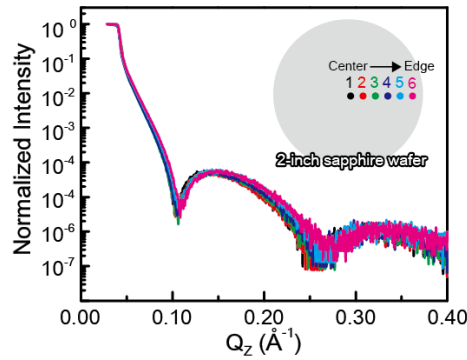


Figure S1-2. XRR spectra of the few-layer h-BN film grown by MOCVD measured at six different positions in a single wafer.

3) Self-termination effect

Figure S1-3 shows the X-ray reflectance spectrum of the h-BN films whose pulse cycle numbers are 100 and 200, respectively. Red open circles in Figure S1 indicate the calculated reflectivity. The Estimated film thicknesses are 2.6nm for h-BN whose pulse cycle is 100, and 2.0nm for h-BN whose pulse cycle is 200. Film thickness doesn't increase even the prolonged the pulse cycle, i.e., longer growth time which is due to the self-termination effect occurring when V/III ratio is very high and reactor pressure is low^{S2,S3}.

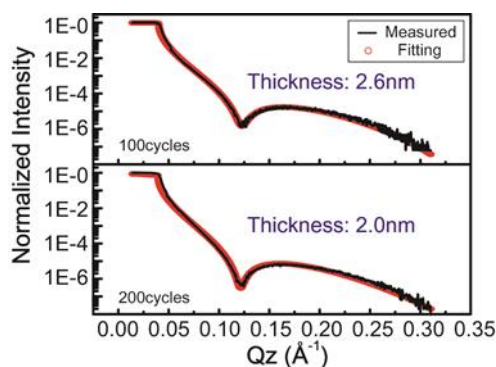


Figure S1-3. X-ray reflectance (XRR) spectrum. XRR spectrum of the h-BN films whose pulse cycles are 100 and 200, respectively. Black line indicates measured value and red open circle shows the fitted value.

Supporting Information S2. Average tilt angle

Layered structure of the grown h-BN films are qualitatively discussed in the manuscript based on the cross-section TEM image and the angle-dependent NEXAFS spectra. The degree of the h-BN layer alignment parallel to the surface is expressed quantitatively by the average tilt angle which can be calculated from the angle-dependent NEXAFS spectra.

Theoretically, optical transition probability is proportional to the square of the transition matrix element, $|M_T|^2$, which is expressed as

$$|M_T|^2 = |\langle f | \hat{e} \cdot \mathbf{p} | i \rangle|^2$$

where, f and i are the final and initial states associated in the optical transition, respectively, \hat{e} is the basis function, and \mathbf{p} is the polarization of light. For the NEXAFS K-edge spectroscopy, the initial state is $1s$ which is isotropic. Therefore, the intensity of the spectrum is dependent on the final state and the polarization of the incident X-ray which can be controlled by the incident angle of X-ray source since the synchrotron radiation is linearly polarized.

Let us consider the optical transition from $1s$ to π^* states in h-BN atomic layers aligned parallel to the surface. Since π^* orbitals are vertically aligned to the atomic plane, optical transition is maximized when the polarization of light is also vertical to the atomic plane which corresponds to a low incident angle. In contrast, optical transition is forbidden when the polarization of light is parallel to the surface, that is, when X-ray is incident to normal to the surface as shown in Figure S2-1.

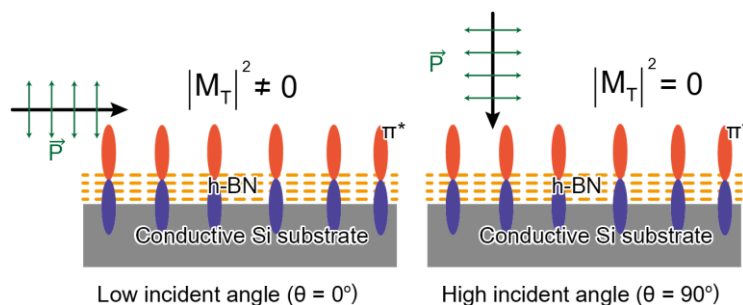


Figure S2-1. Incident-angle-dependent optical transition matrix for NEXAFS spectroscopy.

More precisely, optical transition probability from $1s$ to π^* is proportional to the cosine squared X-ray incident angle which is expressed as follow^{S3}.

$$I = C \cdot \frac{P}{3} \left\{ 1 + \frac{1}{2} (3\cos^2\theta - 1)(3\cos^2\alpha - 1) \right\} + \frac{(1 - P)}{2} \sin^2\alpha$$

where, C is the constant, P is the polarization ratio, θ is the polarization angle of the incident X-ray with respect to surface normal direction, and α is the average tilt angle of the atomic planes. Based on the above equation, the average tilt angle can be calculated as shown in Figure S2. Since the polarization ratio is constant, θ is known value, and I is the measured data, one can find C and α that reproduce the experimental results well. Red open circles are maximum intensity of π^* peak in NEXAFS B K-edge shown in Figure 2(a) in the manuscript and black solid line is the best fitting result. The obtained average tilt angle is approximately 21.2° which is attributed to the structural imperfections in the h-BN film as briefly discussed in the manuscript.

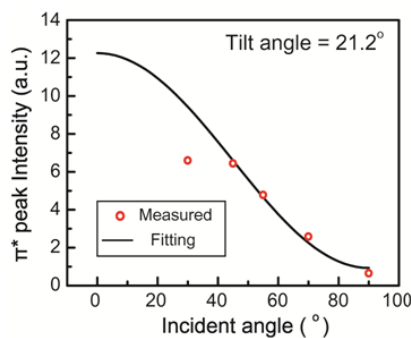


Figure S2-2. Intensity of π^* peak in NEXAFS B K-edge spectrum as a function of X-ray incident angle (red open circle) and the calculated intensity (black line) for estimation of the average tilt angle.

Supporting Information S3. Surface morphology of h-BN films grown at different pressures

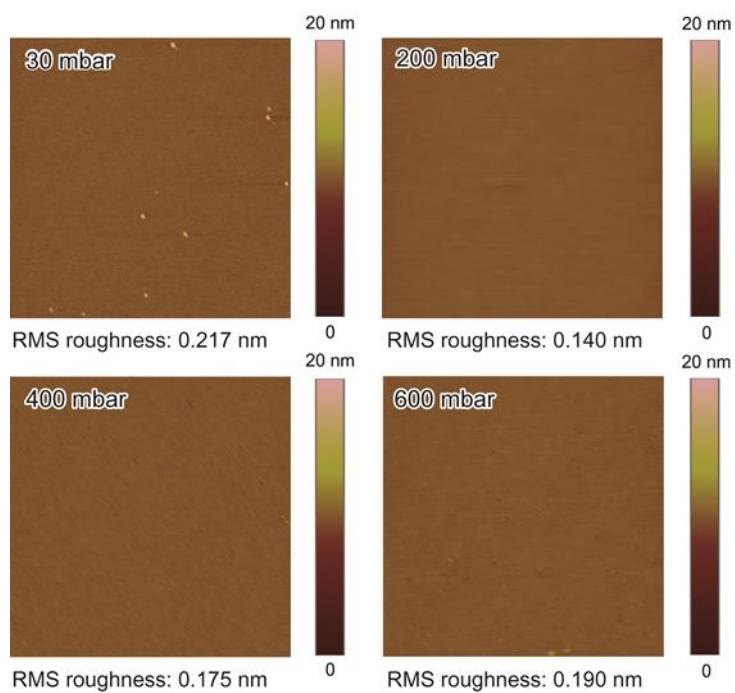


Figure S3. AFM images. Surface morphologies of the h-BN films grown at different reactor pressures in a scanning area of $5 \mu\text{m} \times 5 \mu\text{m}$. Surface roughness is around 0.2 nm for all the films.

Supporting Information S4. NEXAFS spectrum

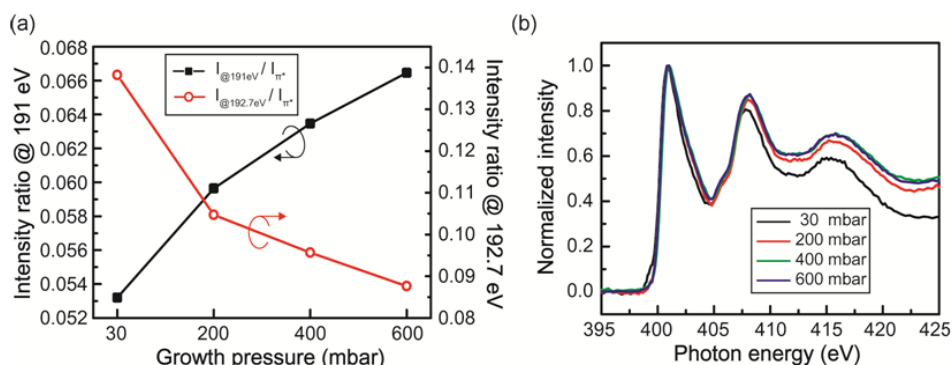


Figure S4. NEXAFS spectrum. (a) Intensity ratio of shoulder peaks and π^* peak in NEXAFS B K-edge spectrum as a function of reactor pressure. Black line and red line with symbols indicates change in intensity ratio of low-energy shoulder and π^* peak, and that of high-energy shoulder and π^* peak, respectively. (b) NEXAFS N K-edge spectrum of the h-BN films grown at different reactor pressures.

Figure S4(a) shows the changes in relative intensity of the shoulder peaks to intensity of π^* peak in NEXAFS B K-edge spectrum. As the pressure increases, the high-energy shoulder at 192.7 eV decreases while the low-energy shoulder at 191.0 eV increases as discussed in the text. In contrast, there is no significant change in NEXAFS N K-edge of h-BN films, even under different reactor pressure conditions as seen in Fig. S4(b).

References

- (S1) Braun, C.; *Parratt32*; Hahn-Meitner-Institut Berlin, Berlin, 1997
- (S2) Paduano, Q. S.; Snure, M.; Bondy, J.; Zens, T. W. C.; Self-terminating growth in hexagonal boron nitride by metal organic chemical vapor deposition, *Appl. Phys. Expr.* **2014**, 7, 071004.
- (S3) Paduano, Q.; Snure, M.; Weyburne, D.; Kiefer, A.; Siegel, G.; Hu, J.; Metalorganic chemical vapor deposition of few-layer sp^2 bonded boron nitride film. *J. Cryst. Growth* **2016**, 449, 148-155.
- (S4) Stöhr, J.; Outka, D. A.; Determination of molecular orientations on surfaces from the angular dependence of near-edge x-ray-absorption fine-structure spectra. *Phys. Rev. B* **1987**, 36, 7891-7905